



A comparison of time-scales governing the interaction and growth of hydrogen bubbles with a solidifying front[☆]



Shyamprasad Karagadde^{a,*}, Pradip Dutta^b

^a Department of Mechanical Engineering, Indian Institute of Technology Bombay, Mumbai 400076, India

^b Department of Mechanical Engineering, Indian Institute of Science, Bangalore 560012, India

ARTICLE INFO

Available online 22 October 2016

Keywords:

Engulfment
Bubble elongation
Microporosity
Scaling
Solidification

ABSTRACT

Elongated hydrogen porosity appears in aluminum based cast components and can lead to crack initiation. In this study, a comparison between the growth rates of hydrogen bubbles and the solidifying front during the process of engulfment is presented. Extending upon a previously developed order estimate for the ratio of growth rates of the two interfaces, it is found that dimensionless grouping leads to two distinct time scales that correspond to solidification and hydrogen diffusion. The analysis proves the hypothesized thought-experiment and explains the mechanism of hydrogen bubble elongation. The scaling prediction is also validated with available experimental studies, and shows that the rate of elongation varies directly with the pore radii and inversely with the cooling rates.

© 2016 Elsevier Ltd. All rights reserved.

1. Introduction

The process of light-weighting in automobile and aerospace applications is strongly desired to reduce global fuel consumption and carbon-dioxide emissions by using aluminum and its alloys. Microporosity is a serious concern in manufacturing of these materials, as it severely degrades the quality of critical components. Gas microporosity defects typically consist of hydrogen bubbles entrapped at various locations by the solidifying interfaces. Hydrogen is appreciably soluble in liquid aluminum and is dissolved in the liquid in the presence of moisture. It is then rejected at the solid-liquid (SL) interface during solidification process, leading to increased hydrogen levels and eventual initiation and growth of bubbles. The pressure and diffusion driven growth of these bubbles and their subsequent engulfment by solidifying fronts lead to the formation of gas microporosity, whose sizes vary from a few microns to hundreds of microns [1,2].

The variation in size and shapes of experimentally observed hydrogen porosity has been attributed to casting conditions, as the rate of hydrogen rejection is primarily governed by the solidification rate. Chalmers [3] proposed a speculation of three different pore morphologies based on slow, intermediate and fast cooling rates. It was hypothesized that at intermediate cooling rates, non-spherical bubble growth could take place leading to elongated pore shapes after partial engulfment of bubbles by the solidifying front. Elongated pores can further

reduce the mechanical properties of critical components, compared to spherical porosity.

Several numerical modelling studies have been reported to predict spherical growth behaviour of hydrogen microporosity using a variety of techniques. Although a majority of them primarily employed cellular automata (CA) technique [4–7], and statistical predictions [8–10], few first-principle approaches have also been reported which track the morphology of the hydrogen pore and its interaction with the solidifying front [11–15]. Sun, et al. [15] reported an extensive computational study using a coupled CA and Lattice Boltzmann Method (LBM) approach to predict interaction of columnar dendrites with a solidification front, successfully capturing the entrapment of gaseous bubbles within the dendritic network. This was also validated with in situ experimental observations, wherein elongated porosity is also observed. Although scaling predictions for interfacial growth exist for dendritic growth in various contexts [9,16,17], literature on the growth of multiple interacting phases involving simultaneous evolution of gas-liquid and solid-liquid interfaces is limited. In a recent work by present authors [18,19], a criterion for pore elongation was derived based on an order-of-magnitude comparison between the growth rates of bubble-liquid (BL) and solid-liquid (SL) interfaces. The estimate was based on approximations for solidification time-scale (Lee and Hunt [10,20]) and concentration gradient at the interface (Carlson et al., [9]). A numerical model was also proposed that simulated the bubble growth and engulfment in 2D, and compared with the analytical scaling relations. The analysis showed explicit dependence of the ratio of growth rates on bubble radius and the cooling rate ($K s^{-1}$) expressed in terms of front speed and thermal gradient. The scaling model was validated with experimental observations and bubble elongation was found to occur

[☆] Communicated by A.R. Balakrishnan and T. Basak.

* Corresponding author.

E-mail address: s.karagadde@iitb.ac.in (S. Karagadde).

when the growth rates of SL and BL interfaces are on the same order. This led to the thinking that a comparison between time-scales of bubble growth and solidification can be made based on the order of magnitude analysis [18] and the thought experiment [3].

In this work, we aim to identify and correlate the time-scales that primarily govern the bubble elongation mechanism by extending the scaling analysis presented in [18], where the final formulation was shown in 2D to compare with 2D numerical simulations. In this work, the relations are derived in generic 3D Cartesian coordinates, and extended to obtain the relation between time-scales. Firstly, a modified expression for hydrogen bubble growth rate based on diffusion from the liquid is discussed. The expression for bubble growth velocity is then approximated based on scaling principles to obtain a comparison of orders-of-magnitude of the time-scales for simultaneous solidification and bubble growth. The model is further compared with available experimental data for validation.

2. System description

We consider a representative elementary volume (REV) consisting of a hydrogen bubble in close proximity of a solidifying front. The schematic is shown in Fig. 1. The solid front movement (speed V_{int}^s) in the system (with a length scale L_s) is driven by heat removal from one of the boundaries (left boundary in the schematic). This leads to the rejection of hydrogen into the liquid (due to lower solubility in the solid phase) at the s-l interface. Subsequently, hydrogen concentration in the liquid (C_l) increases compared to the b-l interface concentration C_{lp} . This concentration gradient over a diffusion length scale L_d drives the hydrogen into the bubble and resulting in the bubble growth (with speed V_{int}^p). The planar solidifying interface shown in the schematic also represents an advancing eutectic front or dendritic arm.

3. Hydrogen bubble growth

Consider a bubble of radius R surrounded by liquid supersaturated with hydrogen concentration. The super-saturation causes a positive concentration gradient at the interface to initiate the influx of hydrogen into the bubble. Pressure inside the bubble is given by Young's relation, $P_p = P_0 + \frac{2\sigma}{R}$, where σ is the surface tension and P_0 is the reference pressure. From Lee and Hunt [10] and Pequet et al. [8], the concentration at

the interface is assumed to be governed by Sievert's law which states that interface concentration is proportional to the square root of the bubble pressure, i.e.,

$$C_{lp} = S_l \sqrt{\frac{P_p}{P_0}} \quad (1)$$

where S_l is Sievert's constant or the limit of solubility at the standard pressure. It is expressed as $\log_{10} S_l = 2.256 - 2392/T - 0.0119 \times 0.12$, Sasikumar et al., [5]. The concentration inside the bubble is calculated using the ideal-gas law. A conversion factor is used to relate the number of moles per unit volume of hydrogen inside the bubble in terms of $\text{cm}^3/100 \text{ g}$ of aluminum (Sasikumar et al. [5]). Thus, bubble concentration (C_p) is given by the relation,

$$C_p = C_c \left(\frac{P_p}{\mathfrak{R}T} \right) \quad (2)$$

where $C_c = \left(\frac{\mathfrak{R}T_{sp}}{P_{sp}} \right) \left(\frac{100}{\rho_{Al}} \right)$, density of aluminum $\rho_{Al} = 2.5 \text{ g/cm}^3$ and $\mathfrak{R} = 8.314 \text{ J/mol-K}$ is the Universal Gas Constant. The term C_c converts the number of moles into $\text{cm}^3/100 \text{ g Al}$.

Assuming diffusion dominated growth of hydrogen bubbles, an expression for bubble growth velocity can be obtained. Let R denote the radius of the bubble; and C_p and C_{lp} denote hydrogen concentration inside the bubble and at the BL interface respectively. Referring to Fig. 1, the mass inside the bubble, is given by $\frac{4}{3}\pi R^3 C_p$. Due to growth of the bubble at the rate $\frac{dR}{dt}$, the rate of increase of mass in the inner sphere is given by,

$$\frac{d}{dt} \left[\frac{4}{3}\pi R^3 C_p \right] = 4\pi R^2 C_p \frac{dR}{dt} + \frac{4}{3}\pi R^3 \frac{dC_p}{dR} \frac{dR}{dt} \quad (3)$$

This term is balanced by the following two phenomena.

- (i) the rate of concentration influx toward the boundary due to diffusion, and
- (ii) the rate of flow due to the movement of the boundary; i.e.,

$$4\pi R^2 D_l \frac{\partial C_l}{\partial r} + 4\pi R^2 C_{lp} \frac{dR}{dt} \quad (4)$$

Equating Eqs. (3) and (4) and simplifying, we obtain the expression for interface velocity in the following form,

$$V_{\text{int}}^p = \frac{1}{(C_p - C_{lp} - C_d)} D_l \frac{\partial C_l}{\partial r} \Big|_{r=R} \quad (5)$$

where $C_d = -\frac{R}{3} \frac{dC_p}{dR} = \frac{2\sigma C_c}{(3\mathfrak{R}T)R}$. For a 2D case, the expression simplifies to $-\frac{\sigma C_c}{(2\mathfrak{R}T)R}$ [12,18].

3.1. Growth rate of the solid phase

Rate of growth of solid phase can be written as $V_{\text{int}}^s = \dot{f}_s \times L_s$, where \dot{f}_s is the rate of change of solid fraction and L_s is a length scale of the domain. In this problem, the solidifying front could be located anywhere between 0 and L_s .

3.2. An approximation for the growth rate of the bubble phase

Consider the growth of a hydrogen bubble of radius R_p , schematically shown in Fig. 1. The expression for the interface velocity is given by Eq. (5). First, let us consider the denominator of the Eq. (5) along with their definitions, i.e., $C_{\text{diff}} = C_p - C_{lp} - C_d$. These terms clearly show a

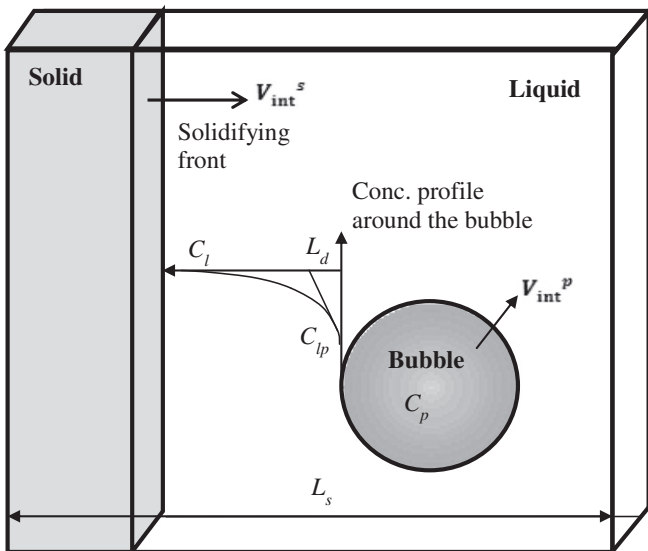


Fig. 1. Schematic of the system under consideration.

Download English Version:

<https://daneshyari.com/en/article/4993041>

Download Persian Version:

<https://daneshyari.com/article/4993041>

[Daneshyari.com](https://daneshyari.com)